

In Vivo Assessment of Brainstem Depigmentation in Parkinson Disease: Potential as a Severity Marker for Multicenter Studies¹

Stefan T. Schwarz, MD, MSc
 Yue Xing, PhD
 Pragya Tomar, MSc
 Nin Bajaj, PhD
 Dorothee P. Auer, PhD

Purpose:

To investigate the pattern of neuromelanin signal intensity loss within the substantia nigra pars compacta (SNpc), locus coeruleus, and ventral tegmental area in Parkinson disease (PD); the specific aims were (a) to study regional magnetic resonance (MR) quantifiable depigmentation in association with PD severity and (b) to investigate whether imaging- and platform-dependent signal intensity variations can be normalized.

Materials and Methods:

This prospective case-control study was approved by the local ethics committee and the research department of Nottingham University Hospitals. Written informed consent was obtained from all participants before enrollment in the study. Sixty-nine participants (39 patients with PD and 30 control subjects) were investigated with neuromelanin-sensitive MR imaging by using two different 3-T platforms and three differing protocols. Neuromelanin-related volumes of the anterior and posterior SNpc, locus coeruleus, and ventral tegmental area were determined, and normalized neuromelanin volumes were assessed for protocol-dependent effects. Diagnostic test performance of normalized neuromelanin volume was investigated by using receiver operating characteristic analyses, and correlations with the Unified Parkinson's Disease Rating Scale scores were tested.

Results:

Reduction of normalized neuromelanin volume in PD was most pronounced in the posterior SNpc (median, -83%; $P < .001$), followed by the anterior SNpc (-49%; $P < .001$) and the locus coeruleus (-37%; $P < .05$). Normalized neuromelanin volume loss of the posterior and whole SNpc allowed the best differentiation of patients with PD and control subjects (area under the receiver operating characteristic curve, 0.92 and 0.88, respectively). Normalized neuromelanin volume of the anterior, posterior, and whole SNpc correlated with Unified Parkinson's Disease Rating Scale scores ($r^2 = 0.25, 0.22, \text{ and } 0.28$, respectively; all $P < .05$).

Conclusion:

PD-induced neuromelanin loss can be quantified across imaging protocols and platforms by using appropriate adjustment. Depigmentation in PD follows a distinct spatial pattern, affords high diagnostic accuracy, and is associated with disease severity.

Published under a CC BY 4.0 license.

Online supplemental material is available for this article.

¹ From the Department of Radiological Sciences, Division of Clinical Neuroscience, School of Medicine (S.T.S., Y.X., P.T., D.P.A.), and The Sir Peter Mansfield Imaging Centre, School of Physics and Astronomy (S.T.S., Y.X., D.P.A.), University of Nottingham, Queen's Medical Centre, Derby Rd, Nottingham NG7 2UH, England; Department of Neurology, Nottingham University Hospitals NHS Trust, Nottingham, England (N.B.); and Department of Radiology, Cardiff and Vale University Health Board, Cardiff, Wales (S.T.S.). Received March 29, 2016; revision requested May 17; revision received July 12; accepted July 25; final version accepted August 26. Address correspondence to S.T.S. (e-mail: stefan.schwarz@nottingham.ac.uk).

This work supported by the Medical Research Council (grant G090132); Parkinson's UK (grant J-1204), support provided to S.T.S and Y.X.; Special Trustees for Nottingham University Hospital (STR 82/04/N); and the Sarah Matheson Trust (now the Multiple System Atrophy Trust founded by Sarah Matheson).

Published under a CC BY 4.0 license.

Parkinson disease (PD) is characterized by a depletion of catecholaminergic neurons in brainstem gray matter nuclei, such as the substantia nigra pars compacta (SNpc), the

Advances in Knowledge

- Neuromelanin-weighted MR imaging sequences with additional magnetization-transfer pulses are sensitive to Parkinson disease (PD)-induced depigmentation of the substantia nigra pars compacta (SNpc) (volume in control subjects, $112.8 \text{ mm}^3 \pm 46.1$; volume in patients with PD, $52.8 \text{ mm}^3 \pm 29.4$; $P < .001$) and locus coeruleus (LC) (volume in control subjects, $16.7 \text{ mm}^3 \pm 9.1$; volume in patients with PD, $11.7 \text{ mm}^3 \pm 6.2$; $P < .05$) but not to neuronal loss in the ventral tegmental area (VTA) (volume in control subjects, $1.3 \text{ mm}^3 \pm 1.6$; volume in patients with PD, 1.5 ± 2.2 [not significant]).
- Variations in MR sequences and imaging unit platforms can be corrected by using sequence-specific signal intensity thresholds, thereby enabling between-site standardized volumetric analysis.
- The most severe PD-induced signal intensity volume loss is found in the posterior SNpc (median, 83%; range, 34%–100%), which correlates well with findings in previous histopathologic studies and shows one of the best receiver operating characteristic (ROC) values (area under the ROC curve, 0.92 ± 0.03 ; $P < .001$) to distinguish patients with PD from healthy control subjects.
- There is a significant inverse correlation of the Unified Parkinson's Disease Rating Scale score (a clinical measure of disease severity) with the signal intensity volume of the anterior ($r^2 = 0.25$, $P < .05$), posterior ($r^2 = 0.22$, $P < .05$), and whole ($r^2 = 0.28$, $P < .05$) SNpc but not that of the LC or the VTA (SNpc volumes corrected for age and cerebral volume).

ventral tegmental area (VTA), and the locus coeruleus (LC) (1). Anatomically, these nuclei can be readily appreciated macroscopically because of a pigment accumulated within the cells called neuromelanin (2). This protein polymer has a molecular structure similar to the skin pigment melanin and is a by-product of catecholamine synthesis. It is deposited within the cells in an age-dependent manner and is largely absent at birth, with accumulation throughout adult life (3,4). There is a PD-induced pathologic decline of SNpc, VTA, and LC neurons that contain neuromelanin, which results in pronounced depigmentation (5,6).

Although the whole of the pars compacta is involved in PD-induced neurodegeneration, the dopaminergic cell loss is nonuniform across its subregions. An area previously described as “ventrolateral” substantia nigra is preferentially and most extensively affected (7). The degree of neuronal loss in the SNpc is correlated to PD severity, which confirms the potential of SNpc imaging in tracking disease progression (8,9). By exploiting the paramagnetic properties of neuromelanin, T1-weighted “neuromelanin-sensitive” magnetic resonance (MR) imaging sequences have been developed to identify and characterize the SNpc and LC in vivo and demonstrate PD-induced signal intensity loss (10,11). Neuromelanin-related MR imaging SNpc signal intensity increase and corresponding loss in PD was confirmed in primates and human specimens postmortem, with good correlation between the density of SNpc neuromelanin that contained neurons and neuromelanin-related MR imaging signal intensity (12,13).



Previous studies also demonstrated the potential of neuromelanin-related SNpc signal intensity loss to index disease progression by showing Hoehn and Yahr stage-dependent changes (14–16). It is unclear whether and how closely neuromelanin-related SNpc signal intensity changes correlate to the Unified Parkinson's Disease Rating Scale (UPDRS) scores as a more accurate estimator of disease severity. How well neuromelanin MR imaging reflects

disease progression and which subregions are most suited to index disease severity also remain unknown.

Additionally, there is lack of standardization, with studies to date varying in acquisition and analysis protocols; this significantly limits the wider clinical use of neuromelanin MR imaging. To the best of our knowledge, there are currently no investigators studying and controlling for the effects of different imaging unit platforms and sequences on neuromelanin-related signal intensity. Being able to compare results independent of different imaging unit platforms or sequences is, however, imperative if this technique is to be used clinically or in multicenter trials.

The purpose of this study was to investigate the pattern of neuromelanin signal intensity loss within the SNpc, LC, and VTA in PD. The specific aims were (a) to study regional MR-quantifiable depigmentation in association with PD severity and (b) to investigate whether imaging- and platform-dependent signal intensity variations can be normalized.

Published online before print

10.1148/radiol.2016160662 Content codes:  

Radiology 2017; 000:1–10

Abbreviations:

AUC = area under the ROC curve
 CI = confidence interval
 LC = locus coeruleus
 MT = magnetization transfer
 PD = Parkinson disease
 ROC = receiver operating characteristic
 SD = standard deviation
 SNpc = substantia nigra pars compacta
 UPDRS = Unified Parkinson's Disease Rating Scale
 VTA = ventral tegmental area

Author contributions:

Guarantors of integrity of entire study, S.T.S., Y.X., D.P.A.; study concepts/study design or data acquisition or data analysis/interpretation, all authors; manuscript drafting or manuscript revision for important intellectual content, all authors; approval of final version of submitted manuscript, all authors; agrees to ensure any questions related to the work are appropriately resolved, all authors; literature research, S.T.S., Y.X., P.T., D.P.A.; clinical studies, S.T.S., N.B., D.P.A.; experimental studies, S.T.S., Y.X.; statistical analysis, S.T.S., Y.X., P.T., D.P.A.; and manuscript editing, S.T.S., Y.X., N.B., D.P.A.

Conflicts of interest are listed at the end of this article.

Materials and Methods

This final analysis was part of a prospective multimodal MR imaging characterization of the SNpc in patients with PD and was approved by the local ethics committee (North Nottinghamshire Research Ethics Committee, United Kingdom, reference no. 05/Q2402/87; Derbyshire Research Ethics Committee, United Kingdom, reference no. 10/H0401/35) and the research department of Nottingham University Hospitals NHS Trust. Data were collected periodically from March 2007 to March 2015. All participants had to be 30 years and older, have undergone the Addenbrooke's Cognitive Examination test battery, and had to have a score higher than 80 for inclusion. All participants had Mini-Mental State examination scores of at least 27. All patients included in the study had to fulfill the UK Brain Bank criteria for a diagnosis of PD and were recruited from movement disorders clinics at two local National Health Service trusts. All control subjects were recruited via spouses and friends and had to be free from movement disorder symptoms. Participants were excluded from the study if there were any contraindications to MR imaging, such as potential intraocular metallic foreign bodies, intracranial aneurysm clips, cardiac pacemakers, defibrillators, or cochlear implants. Of 112 participants enrolled, 76 participants were recruited into the neuromelanin substudy and underwent imaging with any of three prespecified neuromelanin-sensitive MR imaging protocols. Six participants had to be excluded because of severe movement artifacts. One patient was excluded because of change of diagnosis at follow-up (Fig 1). The final study analysis included 39 patients and 30 control subjects. Written informed consent was obtained from all participants before enrollment in the study after undergoing assessment of capacity by a neurology consultant (N.B.). Disease severity was recorded by using the UPDRS and Hoehn and Yahr clinical rating scales for PD (17). Patients were assessed and underwent imaging while medicated. Data from 17 of the 69 participants included in the current study have been reported

Figure 1

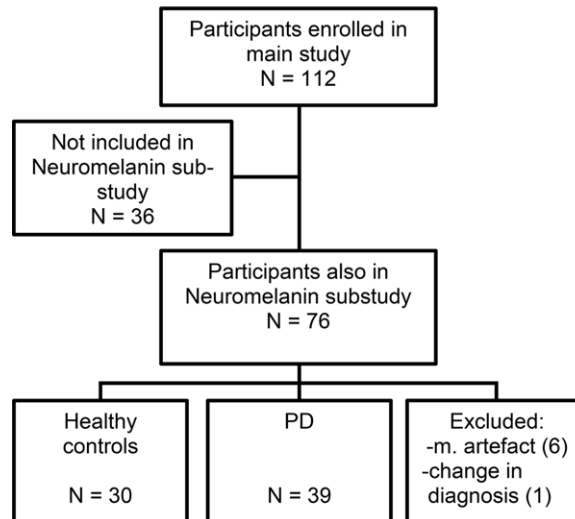


Figure 1: Participant inclusion flowchart. *m.* = movement.

previously (14). The current study expands on the prior study by introducing a new algorithm to adjust for varying neuromelanin-sensitive sequences and imaging unit platforms by introducing a new segmentation technique of the substantia nigra and by relating neuromelanin sub-regional SNpc signal intensity changes to UPDRS scores.

Imaging was performed with two 3-T MR imaging units (Achieva, Philips Medical Systems, Best, the Netherlands; and Discovery MR750, GE Healthcare, Milwaukee, Wis) with eight- and 32-channel head coils, respectively, and three different sequences (spectral presaturation inversion-recovery acquisition with the Philips imaging unit, magnetization-transfer [MT] acquisition with the Philips imaging unit, and MT acquisition with the GE Healthcare imaging unit; Table 1). The orientation of the axial sections was individually aligned parallel to a line that connected the splenium and genu of the corpus callosum. High-spatial-resolution anatomic images were obtained in each individual's brain by using a T1-weighted three-dimensional magnetization-prepared rapid-acquisition gradient-echo sequence (voxel size, 1 mm isotropic).

We modified a previously proposed analysis method to determine hyperintense neuromelanin-rich volumes (S.T.S., a senior clinical research fellow

in neuroradiology with 8 years of experience in movement disorder imaging research) (14,18,19). Suprathreshold hyperintense volumes were assessed on three adjacent sections in the whole SNpc, VTA, and LC. In addition, the SNpc was geometrically divided into anterior and posterior halves by using manually placed regions of interest (anterior and posterior SNpc, performed by S.T.S.). Region of interest placement and signal intensity distribution were determined by using image analysis software (Jim version 7.0, Xinapse Systems, Colchester, United Kingdom; www.xinapse.com). For more details, see Figures E1–E6 (online). Backgrounds were chosen as midbrain tegmentum and cerebral peduncles for the SNpc and VTA, respectively, and the pons for the LC. We averaged the signal intensity obtained from the background regions of interest for calculation of the mean background signal intensity and expressed background noise as the standard deviation (SD) of the background signal intensity.

We determined an adjustment factor for the threshold to define neuromelanin-containing voxels across acquisition protocols and imaging units. We achieved this by identifying a reference protocol out of the three neuromelanin-sensitive MR imaging protocols that best matched the normative volumes from a recent

Table 1

MR Sequences Used to Assess Brainstem Neuromelanin Content of the Substantia Nigra, LC, and VTA

Sequence	Participants	Sequence Parameters
Spectral presaturation inversion-recovery acquisition with the Philips imaging unit	10 control subjects, 12 patients with PD	T1-weighted imaging with spectral presaturation inversion-recovery pulse conferring an MT effect within the specific absorption rate limits (repetition time [msec]/echo time [msec], 688/9; section thickness, 2.5 mm; 0.25-mm gap; 0.47 × 0.47 pixel resolution; four signals acquired, 21 sections; acquisition time, 12 minutes)
MT acquisition with the Philips imaging unit	10 control subjects, 12 patients with PD	Modified version of the above T1-weighted sequence, replacing the spectral presaturation inversion-recovery pulse with a standard Philips "off-resonance" MT pulse (904/9; section thickness, 2.5 mm; 0.25-mm gap; 0.47 × 0.47 pixel resolution; four signals acquired; 12 sections; acquisition time, 12 minutes 34 seconds)
MT acquisition with the GE Healthcare imaging unit	10 control subjects, 15 patients with PD	T1-weighted spin-echo sequence with additional "off-resonance" MT pulse (600/10; section thickness, 2.5 mm; 0.38 × 0.38 pixel resolution; 0.3-mm gap; three signals acquired; 12 sections; acquisition time, 9 minutes 32 seconds)

histologic study (20). We then standardized the group mean SNpc volumes of respective healthy control subjects in the other two groups to the values observed in the reference protocol. The mean overall substantia nigra volume (right and left) in the postmortem study (eight female patients and seven male patients; age range, 50–91 years; mean age ± SD, 67.4 years ± 13.2) was reported as 187.8 mm³ ± 34.1 (20). The substantia nigra consists of approximately 68% pigmented neurons (21), which allowed estimation of a "normal" pigmented substantia nigra volume of 127.7 mm³ ± 23.1.

By choosing a previously published threshold signal intensity method for determination of high-signal-intensity SNpc neurons as a reference (14), we found that determination of neuromelanin-rich volume in the control cohort that underwent MT acquisition with the Philips imaging unit yielded a group mean pigmented SNpc volume of 106.9 mm³ ± 47, which best matched the expected pigmented volume (Fig 2a, *n* = 10 each) (20,21). Threshold signal intensity (THR_{si}) was calculated as follows:

$$\text{THR}_{\text{si}} = \text{BG}_{\text{mean}} + (3 \cdot \text{SD}_{\text{BG}}),$$

where BG_{mean} is the mean background signal intensity and SD_{BG} is the SD of the background signal intensity. The suprathreshold signal intensity volumes with the other two sequences were investigated by using a range of multipliers (one to five times the SD

of the background signal intensity) in healthy control subjects, and for each sequence, we chose a multiplier that was used to adjust the respective control group mean to the signal intensity volume of the reference protocol (Fig 2b; left solid arrow, spectral presaturation inversion-recovery acquisition with the Philips imaging unit [2.75 SD + background signal intensity]; right solid arrow, MT acquisition with the GE Healthcare imaging unit [3.57 SD + background signal intensity]). This enabled us to establish normalized neuromelanin volumes. To examine the accuracy of neuromelanin-weighted MR imaging as a diagnostic test of PD in comparison to control subjects, a receiver operating characteristic (ROC) analysis of subregional neuromelanin volumes was performed before and after protocol-specific threshold signal intensity adjustment.

To further adjust for variations in cerebral volumes, we calculated the total cerebral volumes (hemispheric and subcortical gray and white matter) by using FreeSurfer 5.3 (<https://surfer.nmr.mgh.harvard.edu/>; analysis performed by Y.X., a postdoctoral research fellow with more than 3 years of imaging research in PD).

To visually display the disease stage-dependent depigmentation in PD, we constructed a group-averaged neuromelanin map (Fig 3) by registering neuromelanin images to the high-spatial-resolution anatomic volumes by using "FSL FLIRT," the Oxford Centre

for Functional MRI of the Brain, or FMRIB, linear imaging registration tool (<http://fsl.fmrib.ox.ac.uk/fsl/fslwiki/FLIRT>; Appendix E1 [online]).

Statistical tests (including ROC analyses, linear regression, and analysis of variance) were performed by using IBM-SPSS for windows (version 21.0; IBM, Armonk, NY) and Microsoft Excel 2010 (Microsoft, Redmond, Wash). Group comparisons between patients and control subjects were performed by using univariate or multivariate analysis of variance with least-squares differences post hoc comparison or Student *t* tests. Nonparametric tests were used for group comparisons in case of nonnormal distribution of the data. Values are given as means ± SDs or as medians with interquartile ranges and ranges, unless stated otherwise. Significance was defined at *P* less than .05. ROC analyses and intraclass correlation coefficient analyses (the second measurement performed by Y.X., a blinded investigator) were performed by using SPSS software (for details, see Appendix E1 [online]). Partial correlation analysis was performed by using SPSS and Matlab software version 2015a (<http://www.mathworks.com/products/matlab>; S.T.S. and Y.X.).

Results

There was no difference in age or sex distribution of the patients with PD and the control subjects (patients with PD, 22 men [mean age, 66 years ± 7.6; age

Figure 2

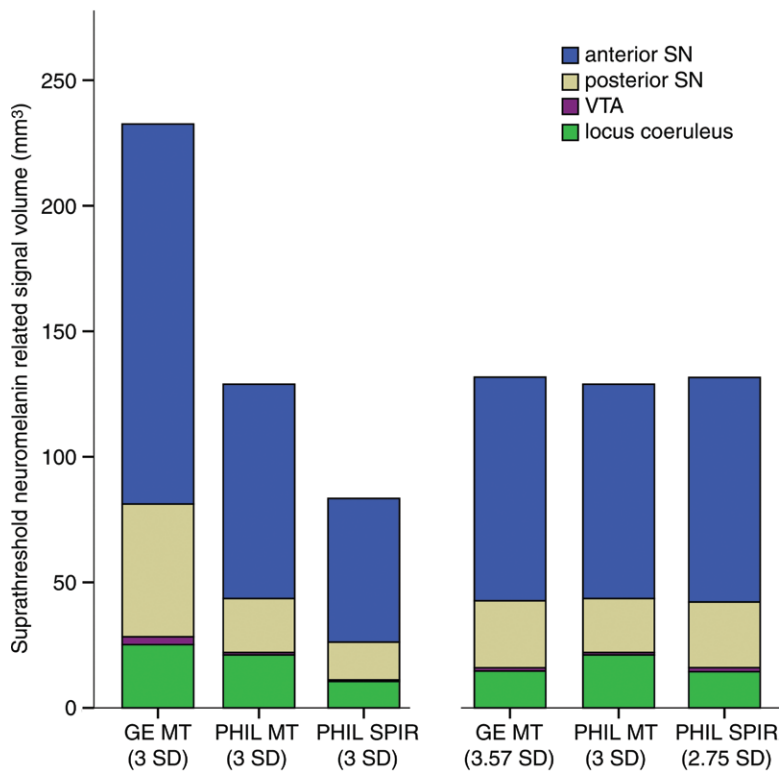
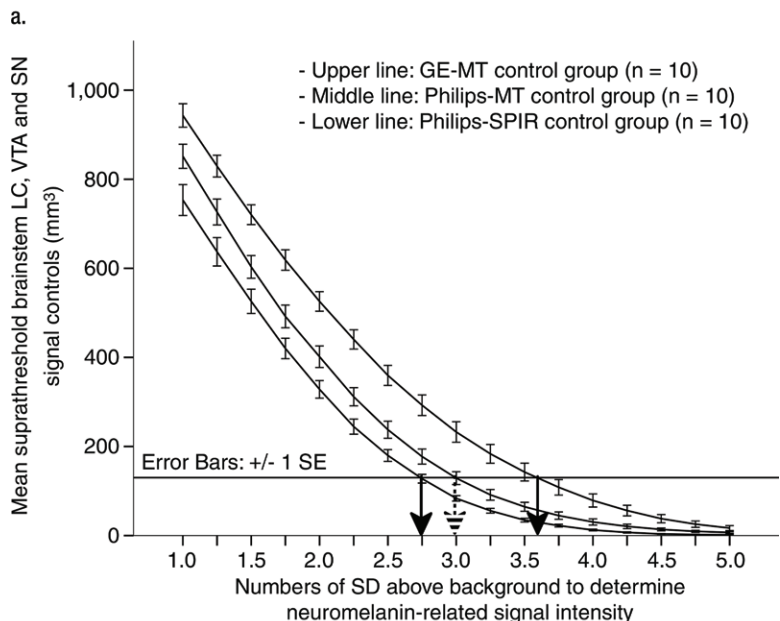


Figure 2: Adjustment to account for MR sequence-dependent neuromelanin-related signal intensity. **(a)** Bar graph shows threshold (given as a multiplier of SD, x-axis) and sequence-dependent brainstem neuromelanin volume (y-axis) in healthy control subjects before (first three bars) and after (last three bars) threshold signal intensity adjustment. **(b)** Graph indicates that by using 3 SDs above mean background signal intensity for the group that underwent MT acquisition with the Philips (PHIL) imaging unit as the reference (striped arrow), the resultant volume allows derivation of the corresponding multipliers for the other sequences (solid arrows). GE = GE Healthcare, SE = standard error, SN = substantia nigra, SPIR = spectral presaturation inversion recovery.



b.

range, 51.8–87.1 years] and 17 women [mean age, 66.5 years ± 11; age range, 41.3–82.8 years]; mean age for all patients with PD, 66.2 years ± 9.1;

control subjects, 17 men [mean age, 63.6 years ± 6.6; age range, 52.2–75.6 years] and 13 women [mean age, 67.7 years ± 7; age range, 59–81.7 years];

mean age for all control subjects, 65.4 years ± 7; for further breakdown of individual groups, see Appendix E1 [online]. Patients with PD had mild to moderate disease severity, with UPDRS scores ranging from 2 to 60 and Hoehn and Yahr stages ranging from 1 to 3 (n = 39; median UPDRS score, 19; median Hoehn and Yahr score, 1.5). The disease duration ranged from 0.1 to 15 years (median, 2 years).

Protocol Dependence and Adjustment Results

The absolute neuromelanin-related signal intensity volume of the brainstem nuclei (sum of substantia nigra, VTA, and LC signal intensities) was dependent on the MR imaging sequence used in the three different control groups. The largest overall hyperintense volume at the fixed threshold (mean + 3 SDs of background signal intensity) was observed in the control group that underwent MT acquisition with the GE Healthcare imaging unit (233 mm³ ± 73), followed by the group that underwent MT imaging with the Philips imaging unit (129 mm³ ± 46); we found the smallest volume in the group that underwent spectral presaturation inversion-recovery acquisition with the Philips imaging unit (83 mm³ ± 19; n = 10 in each group; $F_{(2,29)} = 22.7$; $P < .001$). There was also sequence dependence of the neuromelanin-related volumes of the individual nuclei of anterior and posterior SNpc, LC, and VTA (multivariate analysis, Wilks $\lambda F_{(10,46)} = 4.6$; $P < .001$; with post hoc analysis,

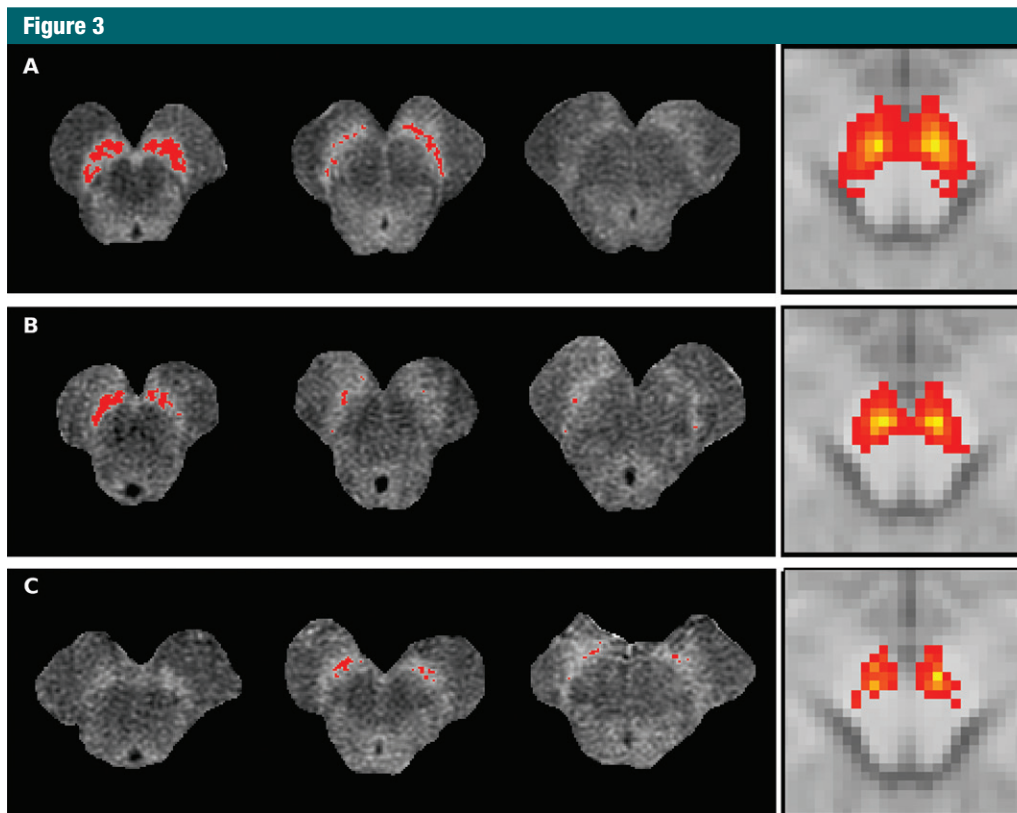


Figure 3: Left images show examples of consecutive brainstem neuromelanin-weighted axial MR images and superimposed suprathreshold neuromelanin-rich voxels in, *A*, a 63.7-year-old female control subject, *B*, a 64.3-year-old male patient with mild PD and a UPDRS score of 19, and, *C*, a 70.8-year-old male patient with moderate PD and a UPDRS score of 47. Right images represent group average maps of concatenated nigral neuromelanin-rich voxels projected on a T1 atlas image for control subjects (top), patients with mild PD (UPDRS score < 20, middle), and patients with moderate PD (UPDRS score \geq 20, bottom).

all subregions were significantly different; see Fig 2a). After threshold adjustment as described earlier, there was no significant difference in hyperintense volumes of the brainstem nuclei nor in the distribution of hyperintense volumes within the anterior and posterior SNpc, VTA, and LC ($F_{(10,46)} = 0.7$; $P = .41$; with post hoc analysis, there was no significant difference between subregions; lowest P value, $P = .18$ in the LC region; Fig 2a). By using normalized signal intensity volumes, we found a mild negative correlation of the signal intensity volume of the anterior SNpc with age in all control subjects ($r^2 = 0.14$; $F_{1,29} = 4.5$; $P = .04$) but not in the PD group (anterior SNpc, $P = .94$) or in the other brainstem regions (for control subjects the lowest P value was $P = .08$ in the posterior SNpc region; for patients with PD the lowest P value was $P = .22$ in

the LC region). There was no significant correlation of cerebral volumes with any of the brainstem nuclei neuromelanin volumes in the healthy control group (lowest P value, $P = .48$ in the LC region) or the PD group (lowest P value, $P = .30$ in the whole SNpc region). The intraclass and interclass correlation coefficients for intrarater and interrater concordance were very high, with correlation coefficients of 0.99 (95% confidence interval [CI]: 0.97, 0.99) and 0.94 (95% CI: 0.90, 0.97; all $P < .001$), respectively.

Diagnostic Performance of Normalized and Nonnormalized Regional Neuromelanin Volume

The sequence-specific normalization procedure significantly improved the diagnostic test performance of using regional neuromelanin measures as

markers of PD (Fig 4). The area under the ROC curve (AUC) for the normalized (threshold-adjusted) posterior and whole SNpc neuromelanin-rich volumes demonstrated the best distinction between patients with PD and control subjects (posterior SNpc, adjusted AUC \pm standard error of 0.92 ± 0.03 [$P < .001$], nonadjusted AUC of 0.82 ± 0.05 [$P < .001$], and $z = -2.72$ [$P = .006$] for adjusted AUC vs nonadjusted AUC [22]; whole SNpc, adjusted AUC of 0.88 ± 0.04 [$P < .001$], nonadjusted AUC of 0.76 ± 0.06 [$P < .001$], and $z = -2.56$ [$P = .01$] for adjusted AUC vs nonadjusted AUC). Measurements in the anterior SNpc and the LC demonstrated good to moderate AUC values when values adjusted for threshold signal intensity were used (AUC \pm standard error, 0.82 ± 0.05 [$P < .001$] and 0.67 ± 0.07 [$P = .02$], respectively) with

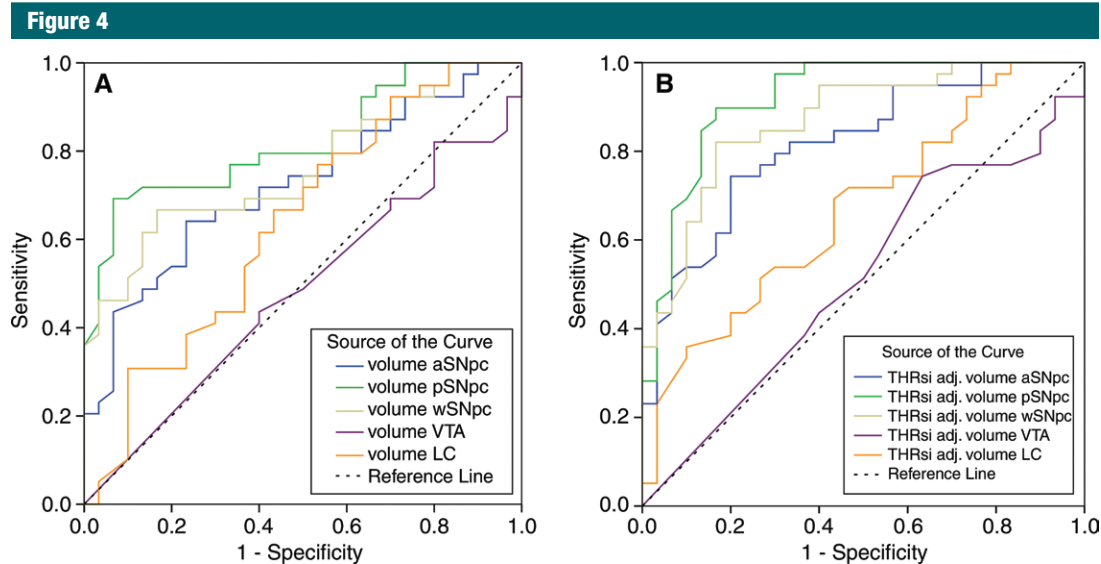


Figure 4: ROC analysis of pigmented volumes of midbrain nuclei was conducted to diagnose PD, *A*, before and, *B*, after normalization by using sequence-specific threshold adjustments. Diagonal segments are produced by ties. *adj.* = adjusted, *aSNpc* = anterior SNpc, *pSNpc* = posterior SNpc, *THRsi* = threshold signal intensity, *wSNpc* = whole SNpc.

poorer performance when using values not adjusted for threshold signal intensity (AUC \pm standard error for anterior SNpc, 0.72 ± 0.06 ; LC, 0.64 ± 0.7 ; adjusted vs nonadjusted AUC, $z = -2.1$ [$P = .02$] and $z = 0.38$ [$P = .7$], respectively). VTA volumes did not allow separation of the groups (adjusted AUC \pm standard error, 0.51 ± 0.07 ; nonadjusted AUC \pm standard error, 0.48 ± 0.07).

Comparing the diagnostic test performances of the adjusted individual SNpc regions and the LC as disease classifiers demonstrated that the highest AUC value of the posterior SNpc was not significantly different from that of the whole SNpc ($z = 1.03$, $P = .30$). There was, however, a significant difference when comparing the AUC of the posterior and whole SNpc with the AUC of the anterior SNpc and LC (lowest z value, $z = 2.1$; $P = .04$).

The optimal cutoff value of posterior and whole SNpc volumes to differentiate patients with PD and control subjects with the highest sensitivity and specificity was determined to be 10.72 mm^3 for posterior SNpc and 72.98 mm^3 for whole SNpc. When using the posterior SNpc value for classification, it was used to differentiate patients with PD and control subjects with a

sensitivity of 89.7% (35 of 39 patients; 95% CI: 80.1%, 99.2%) and a specificity of 83.3% (25 of 30 control subjects; 95% CI: 70%, 96.6%). When using the whole SNpc value for classification, it was used to differentiate patients with PD and control subjects with a sensitivity of 82.0% (32 of 39 patients, 95% CI: 70%, 94.1%) and a specificity of 83.3% (25 of 30 control subjects; 95% CI: 70%, 96.6%).

Pattern of Neuromelanin in Healthy Aging and PD

In healthy control subjects, most of the neuromelanin-related signal intensity in the SNpc was located anteriorly (mean \pm SD, $78\% \pm 10$ vs $22\% \pm 9$ posteriorly; $P < .001$). The relative distribution of anterior and posterior SNpc volumes was independent of the MR imaging sequence ($F_{(2,29)} = 0.89$, $P = .43$). In patients with PD, the relative signal intensity content of the posterior SNpc was smaller than that in control subjects (patients with PD, $13\% \pm 11$; median, 11%; interquartile range, 4%–17%; range, 0%–60%; Mann Whitney U test for patients vs control subjects, $P < .001$). In comparison to control subjects, patients with PD showed a significant reduction in normalized

neuromelanin-related volumes of the anterior, posterior, and whole SNpc and the LC (Table 2). The PD-related neuromelanin signal intensity loss showed a regional pattern, with the most pronounced median signal intensity loss of 83% in the posterior SNpc (interquartile range, 56%–92%; range, 34%–100%). We found a median reduction of 56% in neuromelanin-rich volumes in the whole SNpc (interquartile range, 42%–68%; range, –10% to 97%), a median reduction of 49% in the anterior SNpc (interquartile range, 23%–63%; range, –30% to 99%), and a median reduction of 37% in the LC (interquartile range, 0%–54%; range, –79% to 77%) in our investigated patient group, with mild to moderately severe PD (Figs 3, 5). The hyperintensity within the VTA region was small, with no significant group difference (threshold signal intensity adjusted for control subjects, $1.3 \text{ mm}^3 \pm 1.6$; threshold signal intensity adjusted for PD, $1.5 \text{ mm}^3 \pm 2.2$; $P = .61$).

Neuromelanin Loss and Disease Severity

There was a borderline nonsignificant correlation of Hoehn and Yahr score with normalized neuromelanin volume of the whole SNpc ($r = -0.31$, $P = .051$),

Table 2

Normalized Neuromelanin-related Volumes of Brainstem Nuclei in Patients with PD and Control Subjects

Nuclei	Control Subjects (n = 30)	Patients with PD (n = 39)	PValue*
Anterior SNpc (mm ³)	87.9 ± 37.7 (80.2) [31.5–160.4]	47.3 ± 26.6 (44.1) [1.2–117.3]	<.001
Posterior SNpc (mm ³)	24.8 ± 16 (23.6) [2–72.8]	5.5 ± 4.51 (4.9) [0–19]	<.001
Whole SNpc (mm ³)	112.8 ± 46.1 (106.9) [44.9–204.1]	52.8 ± 29.4 (49.8) [3–127]	<.001
LC (mm ³)	16.7 ± 9.1 (14.4) [4.5–38.9]	11.7 ± 6.2 (10.3) [1.6–27.9]	.02
VTA (mm ³)	1.3 ± 1.6 (0.7) [0–5.7]	1.5 ± 2.2 (0.61) [0–9.3]	.88

Note.—Data are means ± SDs, unless indicated otherwise. Numbers in parentheses are median values. Numbers in brackets are ranges.

* According to the Mann-Whitney U test.

and there was no significant correlation with the LC ($P = .15$, Pearson correlation). We found a significant mild to moderate negative correlation of UPDRS score with normalized neuromelanin volume, controlled for cerebral volume and age in the anterior SNpc ($r = -0.48$, $P = .003$), posterior SNpc ($r = -0.45$, $P = .007$), and whole SNpc ($r = -0.50$, $P = .002$; Figs 3, 6) but not in the LC or VTA ($P = .24$ and $.44$, respectively; Pearson correlation). There was no significant correlation of disease duration with any of the brainstem nuclei neuromelanin signal intensity when corrected for age (lowest P value, $P = .16$).

Discussion

This current study confirms that neuromelanin-weighted MR imaging is sensitive for PD-induced brainstem depigmentation. We describe preferential neuromelanin-rich volume loss in the posterior SNpc, followed by the anterior SNpc and the LC. Assessment for neuromelanin-related signal intensity loss in the whole or posterior SNpc yielded the best classification characteristics to distinguish patients with PD and control subjects. SNpc depigmentation was mild to moderately correlated with disease severity in a patient cohort with mild to moderate disease. Moreover, we demonstrated how to effectively adjust for protocol-specific neuromelanin signal intensity differences. Neuromelanin MR imaging has potential as a tool for monitoring PD severity-related changes, even when using

different protocols and varying 3-T MR imaging setups, and it holds promise as a useful biomarker for clinicians and in clinical trials.

Use of a previously unpublished normalization algorithm yielded pigmented SNpc volumes in healthy control subjects that closely matched true in vitro SNpc volume measurements from postmortem studies. We achieved improved diagnostic accuracy not only when compared with unadjusted volumetry but also when compared with single-center studies (11,23,24). As a further quantitative validation of our neuromelanin analysis, we note that the preferential volume loss in the region of the posterior substantia nigra compares well to histologic findings of PD-induced cell loss of in the lateral ventral tier described by Fearnly and Lees (25). However, despite the most significant signal intensity loss and the best ROC curves of the posterior and whole SNpc measures, there was an overlap of volumes in patients with PD and control subjects. The number of pigmented brainstem neurons and the SNpc volumes vary greatly, even in a healthy population within a certain age range (20). The overlap observed may be a reflection of true interindividual differences in nigral pigmented volumes. However, the relative variance of SNpc volumes in control subjects observed in the present study by using threshold-adjusted neuromelanin MR imaging is more than double the relative variance in control subjects in histologic studies. Therefore, it is conceivable that the

Figure 5

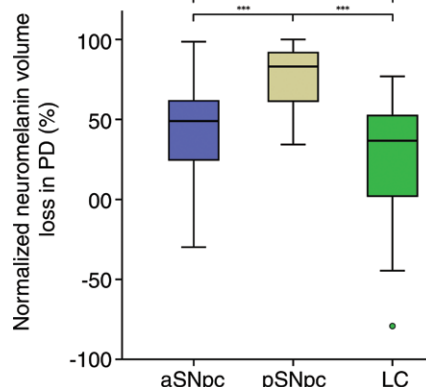


Figure 5: Box and whisker plot illustrates the region-specific depigmentation (normalized neuromelanin volume loss) in patients with PD. The volume reduction in the posterior SNpc (pSNpc) is larger than that in the other pigmented brainstem regions. aSNpc = anterior SNpc. * = $P < .05$, *** = $P < .001$, according to the Wilcoxon rank sum test.

precision of neuromelanin MR imaging techniques in tracking the volume of pigmented brainstem nuclei can be improved further.

Even after controlling for cerebral volume and age, we found significant correlation of neuromelanin volumes in both anterior and posterior SNpc with disease severity, as measured with the UPDRS. This is well in line with previous observations of increased neuromelanin loss with more advanced disease, with Hoehn and Yahr stages a less accurate measure of disease severity (11,14,15,26). In contrast to our finding, a recent study in which an automated SNpc segmentation algorithm was used did not yield a correlation of the substantia nigra volume with the motor UPDRS (27), which might relate to technical differences. There was no correlation of LC volume with measures of disease severity, which is in line with postmortem studies that demonstrated LC cell loss independent of disease duration (28–30). The absolute degree of postmortem LC cell loss found is relatively more (approximately 60% more) (28) than the LC signal intensity loss we or other groups observed (10,27). A potential

Figure 6

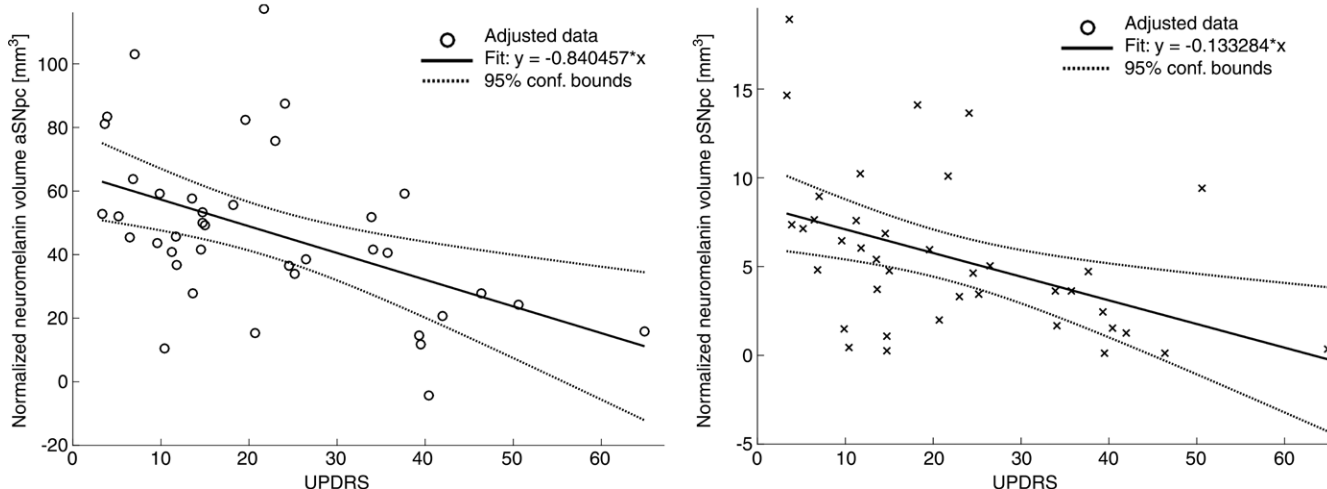


Figure 6: Scatterplots demonstrate the variability of anterior SNpc (*aSNpc*) and posterior SNpc (*pSNpc*) volume in relation to UPDRS score. The substantia nigra volumes are corrected for age and cerebral volume. The dotted lines represent the computed borders of the variability of the mean anterior SNpc and posterior SNpc volume by 2 SDs (95% CI) in relation to UPDRS score.

explanation is the limited resolution of MR imaging for accurate quantification of signal intensity in this small nucleus. This and the lower density of pigmented dopaminergic cells in the VTA (31) will explain the lack of observed VTA changes. A further possible reason for reduced sensitivity in the detection of PD-induced LC and VTA depigmentation may come from the fact that we optimized the threshold for definition of pigmented SNpc.

A limitation of this study is the small sample size of the cohorts investigated. Also, ideally, a single control group in which the three different sequences are used to assess MR imaging sequence-dependent signal intensity alterations should be investigated; however, this is often not a feasible option for multicenter studies. Therefore, our approach of using an age- and sex-matched control group to adjust for sequence-inherent neuromelanin contrast and noise differences is a pragmatic and relevant approach that allows comparison and combination of data sets recorded with different sequences and varying platforms on limited-sample size normative data sets. The observed mild to moderate correlation with disease severity highlights the potential of

neuromelanin volumetry as a progression marker, but longitudinal studies that include large patient cohorts are needed to assess the performance of neuromelanin MR imaging to directly track disease progression.

In conclusion, neuromelanin-weighted MR imaging sequences performed at 3 T are sensitive for PD-induced depigmentation of the SNpc, with excellent diagnostic accuracy for posterior and whole SNpc (AUC, 0.92 and 0.88, respectively) and may offer a progression marker in mild to moderate PD. The proposed threshold adaptation for volumetric analysis allows correction for variations in acquisition protocols as a critical step toward advancing neuromelanin MR imaging techniques for clinical use. Longitudinal studies are now warranted to confirm the potential of neuromelanin-weighted MR imaging as a marker of disease progression for multicenter trials.

Acknowledgments: We thank the PD research study nurses of the Derby Hospitals NHS Foundation Trust for support with participant recruitment and assessment, and we thank all study volunteers for their participation. We acknowledge Penny Gowland, PhD, for useful discussions and confounding of the study.

Disclosures of Conflicts of Interest: S.T.S. disclosed no relevant relationships. Y.X. disclosed no relevant relationships. P.T. disclosed no

relevant relationships. N.B. disclosed no relevant relationships. D.P.A. disclosed no relevant relationships.

References

- Greenfield JG, Bosanquet FD. The brainstem lesions in Parkinsonism. *J Neurol Neurosurg Psychiatry* 1953;16(4):213-226.
- Bazelon M, Fenichel GM, Randall J. Studies on neuromelanin. I. A melanin system in the human adult brainstem. *Neurology* 1967; 17(5):512-519.
- Zucca FA, Bellei C, Giannelli S, et al. Neuromelanin and iron in human locus coeruleus and substantia nigra during aging: consequences for neuronal vulnerability. *J Neural Transm (Vienna)* 2006;113(6):757-767.
- Halliday GM, Fedorow H, Rickert CH, Gerlach M, Riederer P, Double KL. Evidence for specific phases in the development of human neuromelanin. *J Neural Transm (Vienna)* 2006;113(6):721-728.
- Lees AJ, Selikhova M, Andrade LA, Duyckaerts C. The black stuff and Konstantin Nikolaevich Tretiakoff. *Mov Disord* 2008;23(6):777-783.
- Uhl GR, Hedreen JC, Price DL. Parkinson's disease: loss of neurons from the ventral tegmental area contralateral to therapeutic surgical lesions. *Neurology* 1985;35(8):1215-1218.
- Gibb WR, Lees AJ. Anatomy, pigmentation, ventral and dorsal subpopulations of the substantia nigra, and differential cell death in Parkinson's disease. *J Neurol Neurosurg Psychiatry* 1991;54(5):388-396.

8. Ma SY, Røyttä M, Rinne JO, Collan Y, Rinne UK. Correlation between neuromorphometry in the substantia nigra and clinical features in Parkinson's disease using disector counts. *J Neurol Sci* 1997;151(1):83–87.
9. Kordower JH, Olanow CW, Dodiya HB, et al. Disease duration and the integrity of the nigrostriatal system in Parkinson's disease. *Brain* 2013;136(Pt 8):2419–2431.
10. Sasaki M, Shibata E, Tohyama K, et al. Neuromelanin magnetic resonance imaging of locus ceruleus and substantia nigra in Parkinson's disease. *Neuroreport* 2006;17(11):1215–1218.
11. Ohtsuka C, Sasaki M, Konno K, et al. Changes in substantia nigra and locus coeruleus in patients with early-stage Parkinson's disease using neuromelanin-sensitive MR imaging. *Neurosci Lett* 2013;541:93–98.
12. Kitao S, Matsusue E, Fujii S, et al. Correlation between pathology and neuromelanin MR imaging in Parkinson's disease and dementia with Lewy bodies. *Neuroradiology* 2013;55(8):947–953.
13. Bolding MS, Reid MA, Avsar KB, et al. Magnetic transfer contrast accurately localizes substantia nigra confirmed by histology. *Biol Psychiatry* 2013;73(3):289–294.
14. Schwarz ST, Rittman T, Gontu V, Morgan PS, Bajaj N, Auer DP. T1-weighted MRI shows stage-dependent substantia nigra signal loss in Parkinson's disease. *Mov Disord* 2011;26(9):1633–1638.
15. Kashihara K, Shinya T, Higaki F. Neuromelanin magnetic resonance imaging of nigral volume loss in patients with Parkinson's disease. *J Clin Neurosci* 2011;18(8):1093–1096.
16. Matsuura K, Maeda M, Yata K, et al. Neuromelanin magnetic resonance imaging in Parkinson's disease and multiple system atrophy. *Eur Neurol* 2013;70(1-2):70–77.
17. Fahn S, Jenner P, Marsden CD, et al. The Unified Parkinson's Disease Rating Scale. In: Fahn S, Marsden CD, Calne DB, et al, eds. *Recent developments in Parkinson's disease*. Florham Park, NJ: Macmillan Healthcare Information, 1987.
18. Chen X, Huddlestone DE, Langley J, et al. Simultaneous imaging of locus coeruleus and substantia nigra with a quantitative neuromelanin MRI approach. *Magn Reson Imaging* 2014;32(10):1301–1306.
19. Murty VP, Shermohammed M, Smith DV, Carter RM, Huettel SA, Adcock RA. Resting state networks distinguish human ventral tegmental area from substantia nigra. *Neuroimage* 2014;100:580–589.
20. Di Lorenzo Alho AT, Suemoto CK, Polichiso L, et al. Three-dimensional and stereological characterization of the human substantia nigra during aging. *Brain Struct Funct* 2016;221(7):3393–3403.
21. Pakkenberg B, Møller A, Gundersen HJ, Mouritzen Dam A, Pakkenberg H. The absolute number of nerve cells in substantia nigra in normal subjects and in patients with Parkinson's disease estimated with an unbiased stereological method. *J Neurol Neurosurg Psychiatry* 1991;54(1):30–33.
22. Hanley JA, McNeil BJ. A method of comparing the areas under receiver operating characteristic curves derived from the same cases. *Radiology* 1983;148(3):839–843.
23. Ogisu K, Kudo K, Sasaki M, et al. 3D neuromelanin-sensitive magnetic resonance imaging with semi-automated volume measurement of the substantia nigra pars compacta for diagnosis of Parkinson's disease. *Neuroradiology* 2013;55(6):719–724.
24. Reimão S, Pita Lobo P, Neutel D, et al. Substantia nigra neuromelanin magnetic resonance imaging in de novo Parkinson's disease patients. *Eur J Neurol* 2015;22(3):540–546.
25. Fearnley JM, Lees AJ. Ageing and Parkinson's disease: substantia nigra regional selectivity. *Brain* 1991;114(Pt 5):2283–2301.
26. Miyoshi F, Ogawa T, Kitao SI, et al. Evaluation of Parkinson disease and Alzheimer disease with the use of neuromelanin MR imaging and (123)I-metaiodobenzylguanidine scintigraphy. *AJNR Am J Neuroradiol* 2013;34(11):2113–2118.
27. Castellanos G, Fernández-Seara MA, Lorenzo-Betancor O, et al. Automated neuromelanin imaging as a diagnostic biomarker for Parkinson's disease. *Mov Disord* 2015;30(7):945–952.
28. German DC, Manaye KF, White CL 3rd, et al. Disease-specific patterns of locus coeruleus cell loss. *Ann Neurol* 1992;32(5):667–676.
29. Hirsch E, Graybiel AM, Agid YA. Melanized dopaminergic neurons are differentially susceptible to degeneration in Parkinson's disease. *Nature* 1988;334(6180):345–348.
30. Zarow C, Lyness SA, Mortimer JA, Chui HC. Neuronal loss is greater in the locus coeruleus than nucleus basalis and substantia nigra in Alzheimer and Parkinson diseases. *Arch Neurol* 2003;60(3):337–341.
31. Margolis EB, Lock H, Hjelmstad GO, Fields HL. The ventral tegmental area revisited: is there an electrophysiological marker for dopaminergic neurons? *J Physiol* 2006;577(Pt 3):907–924.